Complexes of intrinsic point defects in silicon formed as a result of high-energy xenon ion implantation and post-implantation annealing

© N.A. Maslova¹, D.V. Danilov^{1,2}, O.F. Vyvenko¹, V.A. Skuratov^{3,6,7}, V.A. Volodin^{4,5}, A.E. Kalyadin², N.A. Sobolev²

194021 St. Petersburg, Russia

630090 Novosibirsk, Russia

630090 Novosibirsk, Russia

115409 Moscow, Russia

E-mail: st068118@student.spbu.ru

Received May 5, 2025 Revised July 25, 2025 Accepted July 25, 2025

The depth distribution of point defect complexes in single-crystal silicon irradiated with 167 MeV xenon ions at a dose of $5 \cdot 10^{11}$ cm⁻² and annealed in the temperature range of $400-600\,^{\circ}\text{C}$ is Investigated. We show the formation of a large number of vacancy complexes throughout the implantation region, as well as the presence of a potential barrier at the projection implantation depth. Profiling of the luminescent signal across the wafer depth showed an anomalously large depth of the W/W' line corresponding to interstitial complexes, which is explained by the participation of accelerated diffusion mechanisms in the formation of the distribution of this type of defects

Keywords: Silicon, ion implantation, cathodoluminescence, electron microscopy.

DOI: 10.61011/SC.2025.05.61995.8047

1. Introduction

Ion implantation is used actively in modern microelectronics for modifying the electrical and luminescent properties of silicon, partly owing to the introduction of a large number of radiation-induced defects. In the case of highenergy implantation of heavy ions into a silicon wafer, the irradiation region size may be increased [1,2], which makes it possible to apply a set of electron microscopy methods to examine the depth and the distribution of complexes of point defects. Such studies for MeV heavy ion implantation are virtually absent. At the same time, the interest in the processes of production of intrinsic point defects under these conditions is even growing. It has been demonstrated recently that MeV implantation of xenon into a silicon wafer with subsequent annealing at 400-600 °C leads to the formation of intrinsic interstitial clusters (W centers) [3]. These centers with a narrow zero-phonon luminescence line [4] are among the key candidate sources for a silicon light emitting diode (LED) operating in the infrared (IR) range. Using just such kind of centers, a group of American researchers from the US National Institute of Standards and Technology has recently fabricated a silicon source of IR

radiation and demonstrated its operation in a circuit with a waveguide and a single-photon receiver [5].

2. Methods and materials

An *n*-type silicon wafer with a phosphorus concentration of $10^{15}\,\mathrm{cm}^{-3}$ was studied. It was irradiated with Xe ions with an energy of 167 MeV and a fluence of $5\cdot 10^{11}\,\mathrm{cm}^{-2}$ and subjected to a series of successive 1-h-long thermal annealings in vacuum at temperatures of 400, 500, and $600\,^{\circ}\mathrm{C}$. According to the results of TRIM modeling [6], xenon ions with such energy implanted into silicon are concentrated in a layer with a thickness of $\sim 3\,\mu\mathrm{m}$ at a depth of $\sim 20\,\mu\mathrm{m}$. The large penetration depth provided an opportunity to obtain new data on the depth distribution of emerging defects through the application of a set of methods with standard spatial resolution to bevelled and cross sectional surfaces of the implanted wafer.

To perform electrophysical measurements for an bevelled sample, Schottky diodes with a contact diameter of $800 \,\mu m$ were fabricated by thermal evaporation of gold. With the used angle of 0.5° , this corresponds to a depth resolution

4* 275

¹ St. Petersburg State University,

¹⁹⁹⁰³⁴ St. Petersburg, Russia

² loffe Institute.

³ Joint Institute for Nuclear Research.

¹⁴¹⁹⁸⁰ Dubna, Moscow Region, Russia

⁴ Rzhanov Institute of Semiconductor Physics, Siberian Branch, Russian Academy of Sciences,

⁵ Novosibirsk State University,

⁶ Dubna State University,

¹⁴¹⁹⁸² Dubna, Moscow Region, Russia

⁷ National Research Nuclear University "MEPhl",

of $\sim 7\,\mu\text{m}$. Ohmic contacts were applied to the front and back sides of the wafer by rubbing-in AlGa eutectic alloy in order to measure the electron beam induced current (EBIC). The sample layer damaged due to mechanical processing ($\sim 5\,\mu\text{m}$) was removed by etching in a polishing solution of HF:HNO3 (1:10).

Electrophysical measurements (capacitance-voltage and current-voltage characteristics, CVCs and IVCs) were carried out using Agilent instruments, a Keithley multimeter, and a DLTS SULA Technologies spectrometer. Cathodoluminescence (CL) and EBIC measurements were performed with a Zeiss Supra 40 VP scanning electron microscope and a GatanMonoCL 3+ system equipped with an InGaAs CCD camera and a cooled cryostage. The spatial resolution of these methods is generally defined by the size of the region of generation of electron-hole pairs by an electron beam with account for their diffusion spreading and did not exceed a few micrometers at the accelerating voltages used being quite sufficient in the present case.

3. Results and discussion

Figure 1, a shows the EBIC map obtained at liquid nitrogen temperature. Measurements were carried out in the transverse geometry with the use of ohmic contacts located (relative to the presented map) on the left on the implanted (front) surface and on the right on the back surface of the wafer. In the near-surface layer with a depth up to $20 \,\mu\text{m}$, which corresponds to the region of penetration of implanted ions, a dark band reflecting a reduction in current flowing through the contacts is seen in the EBIC map. At a depth of $\sim 20 \,\mu\text{m}$, the contrast changes sharply. As can be seen from the profile of absolute values of measured current (see the same figure), the light area represents different current directions near the surface $(0-20\,\mu\text{m})$ and in the bulk (20-40 µm): the direction of current with electronhole pairs generated between the surface and the projected implantation depth (R_p) corresponds to the movement of electrons toward the front surface, while the movement toward the back side corresponds to generation in the bulk. This feature, can be attributed in our sample to the presence of a potential barrier at a depth of 20 µm and is similar to the well-known property of grain boundaries [7]. Since impurity xenon is electrically inactive in silicon, the barrier may be induced by damages of the silicon lattice produced by xenon atoms.

The presence of this barrier is also confirmed by the results of examination of the current-voltage curves (Figure 1, b) of the gold Schottky contact applied to the front surface of the wafer. The reverse IVC branches are characterized by saturation and reveal a monotonic increase in current with increasing temperature, which is thermoelectron emission of majority carriers through the Schottky barrier.

The IVC at forward bias and room temperature is also close to that expected of thermoelectron emission. However,

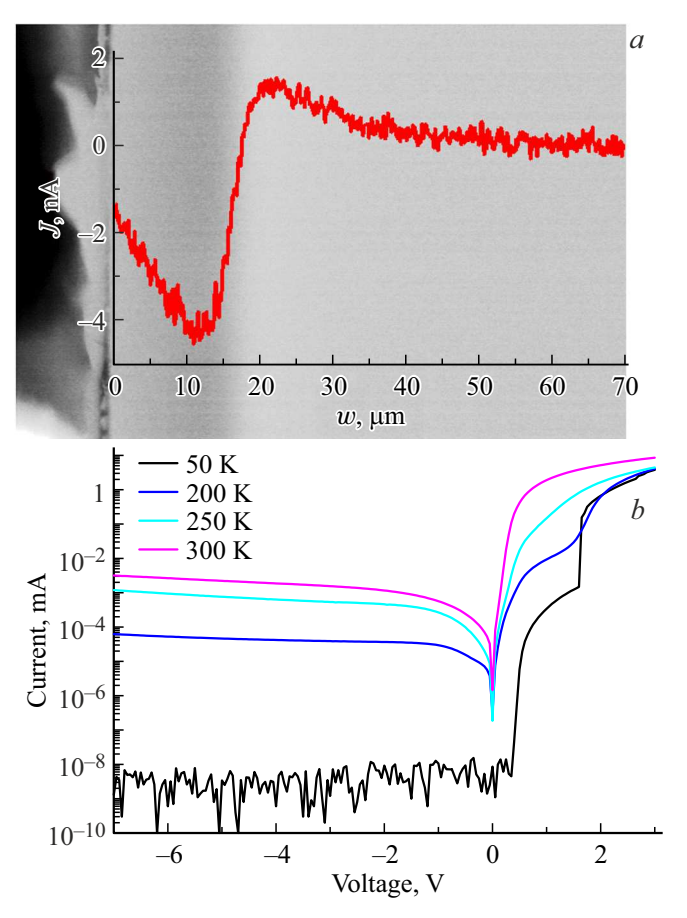


Figure 1. a — EBIC map of the near-surface region of the cross section of the sample with the measured current profile superimposed on it. b — IVCs of the sample at the temperatures of 50-300 K.

as the temperature decreases, a relatively extended section of current saturation emerges within the voltage range of $\sim 0.5-1.5$ V, which indicates the presence of an additional barrier that is connected in series with the Schottky barrier and has its height stabilized by filling of deep levels near the Fermi level. In this case, the voltage at the start of the saturation section must correspond to the condition of equality of both barriers (i.e., to be approximately equal to twice the barrier height). These assumptions are in good agreement with the estimate of barrier height derived from the temperature dependence of current in the saturation region, which was $\sim 0.3 \, \text{eV}$, and with the data of DLTS measurements under the conditions of filling of barrier states, which revealed an intense peak $(E_c - E_t = 0.3 \text{ eV},$ $\sigma_n = 2 \cdot 10^{-15} \, \text{cm}^2$). The defects with the closest emission parameters are divacancies V_2 (--/-) [8]. Their accumulation at depth R_n induces the formation of a barrier in the region of the layer where the majority of implanted atoms are located. The observed patterns are indicative of a qualitative difference between the mechanisms of point defect production at MeV implantation energies and standard energies of several hundred keV: in the latter case, the projected

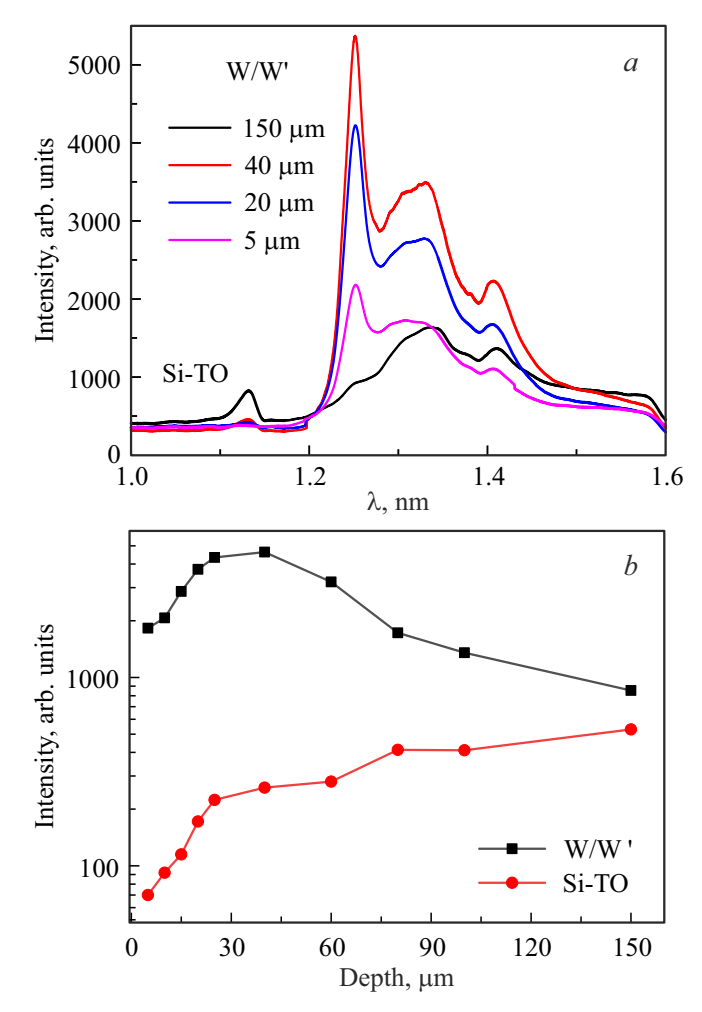


Figure 2. a — CL spectra measured at 68 K in the cross-sectional geometry at chosen points at a distance of $5-150\,\mu\mathrm{m}$ from the implantation surface. b — Distribution of intensity of chosen CL lines with distance to the implantation surface.

implantation depth is the site of accumulation of intrinsic interstitial atoms [2] instead of vacancies.

Figure 2 shows the cathodoluminescence spectra measured at $T = 68 \,\mathrm{K}$ in the cross section of the wafer at points located at the indicated distance from the surface. When silicon is irradiated with 30 keV electrons, 90% of the CL signal is generated in a spot $5\mu m$ in diameter, which was chosen as the minimum step for profiling in the near-surface region. The CL spectra reveal a peak of interband transitions of silicon (Si-TO) at $\sim 1130\,\mathrm{nm}$ and a low-energy band within the range from 1200 to 1600 nm containing several narrow lines. The CL line at 1250 nm is close in position to the radiative transition from the states of interstitial complexes W/W' [3]. Its intensity distribution with sample depth is non-monotonic, which distinguishes it from the distribution profile characteristic of the Si-TO line (see Figure 2, b). In the region of $0-20 \mu m$, the intensity of the Si-TO and W/W' lines increases rapidly with depth. At depths of $20-40 \,\mu\text{m}$, both lines intensify at a slower

rate. This growth is continued at greater depths in the case of the Si-TO line, while the intensity of the W/W' line starts decreasing monotonically as one moves deeper into the sample.

The low intensity of the studied luminescence lines is a consequence of a large number of vacancy deep levels (DLs) detected by DLTS measurements (A-center [9], V_2 (--/-) [8], V_2 (-/0) [10]). Most of these complexes are centers of nonradiative recombination. These DLs were not detected outside the implantation region at a depth of $\sim 40 \,\mu\text{m}$; however, a peak $(0.1 \,\text{eV}/1 \cdot 10^{-16} \,\text{cm}^2)$ corresponding to CiCs complexes, which are a characteristic feature of the formation of intrinsic interstitial complexes [9], was found. This is consistent with the CL data, which revealed that the W/W' line intensity at a depth of $40 \,\mu m$ is 20% higher than its intensity at R_p . The observed shift of the luminescence maximum of this line to a doubled implantation depth may be attributed to a reduction in the number of nonradiative recombination centers in this region, which is evidenced by the identical increase in intensity of the W/W' and Si-TO lines at depths from 20 to $40 \,\mu m$. This correlates with earlier EBIC and DLTS data demonstrating that the barrier at a depth of $20 \,\mu m$ is set by acceptor states of divacancies, which are centers of nonradiative recombination.

One unique finding of the present study is the experimental fact that the W/W' line intensity is nonzero even at a depth of $150\,\mu\mathrm{m}$ (Figure 2, a), which is almost an order of magnitude greater than the projected depth of implantation. Since such a great depth cannot be attributed solely to the peculiarities of the MeV implantation process, it must be inextricably linked to the conditions of subsequent heat treatment. Multi-stage heat processing and the temperatures used indicate that the anomalous depth of these centers may be associated with the effect of accelerated diffusion mechanisms, which involve the motion of entire complexes of interstitial atoms instead of individual atoms of this kind [11,12].

4. Conclusion

A comprehensive study of the distribution of radiation-induced defects in silicon subjected to irradiation with xenon ions with an energy of 167 MeV and subsequent thermal annealing was performed. The presence of vacancy-type complexes within the implantation region and a potential barrier of 0.3 eV at a depth of $\sim 20\,\mu\text{m}$, which corresponds to the depth of xenon ion implantation, was established through the examination of electrophysical characteristics and EBIC measurements. Measurements of cathodoluminescence in the cross section revealed both a drop in luminescence intensity in the implantation region, which is caused by a large number of DL vacancy complexes, and the presence of interstitial complexes producing the W/W' CL line at an anomalously great depth. The obtained results prompted an assumption that accelerated diffusion

mechanisms may affect the distribution of these centers by depth.

Funding

This study was supported by St. Petersburg State University, research project number 125021702335-5.

Acknowledgments

Equipment provided by the Interdisciplinary Resource Center for Nanotechnology of St. Petersburg State University was used in experiments.

Conflict of interest

The authors declare that they have no conflict of interest.

References

- [1] F.F. Komarov. Phys.-Usp., 46 (12), 1253 (2003).DOI: 10.3367/UFNr.0173.200312b.1287
- [2] I. Danilov, H. Boudinov, J.P. de Souza, Yu.N. Drozdov. J. Appl. Phys., 97 (7), 076106 (2005). DOI: 10.1063/1.1886269
- [3] S.G. Cherkova, V.A. Skuratov, V.A. Volodin. Semiconductors, 53 (11), 1427 (2019). DOI: 10.1134/S1063782619110046
- [4] J. Bao, M. Tabbal, T. Kim, S. Chamvanichborikam, A. Kohno, M.J. Aziz. Opt. Express, 15 (11), 6727 (2007). DOI: 10.1364/OE.15.006727
- [5] S. Buckley, J. Chiles, A.N. McCaughan, G. Moody, K.L. Silverman, M.J. Stevens, R.P. Mirin, S.W. Nam, J.M. Shainline. Appl. Phys. Lett., 111 (14), 141101 (2017). DOI: 10.1063/1.4994692
- [6] http://www.srim.org
- [7] D.B. Holt, B. Raza, A. Wojcik. Mater. Sci. Eng. B, **42** (1-3), 14 (1996). DOI: 10.1016/S0921-5107(96)01678-9
- [8] B.G. Svensson, C. Jagodish, A. Hallen, J. Lalita. Nucl. Instrum. Meth. Phys. Res. Section B: Beam Interactions with Materials and Atoms, 106 (1-4), 183 (1995). DOI: 10.1016/J.NIMA.2008.05.046
- [9] S. Libertino, A. La Magna. Materials science with ion beams (Berlin-Heidelberg, Springer Berlin-Heidelberg, 2009)p. 147
- [10] A.V. Vasilev, S.A. Smagulova, S.S. Shaymeev. Sov. Phys. Semicond., 16, 1229 (1982).
- [11] N. Cowern, C. Rafferty. MRS Bulletin, 25 (6), 39 (2000). DOI: 10.1557/mrs2000.97
- [12] R.C. Newman. J. Phys.: Condens. Matter, 12 (25), R335 (2000). DOI: 10.1088/0953-8984/12/25/201

Translated by D.Safin